Indian Journal of Chemistry
Vol. 62, November 2023, pp. 1208-1217
DOI: 10.56042/ijc.v62i11.5091

Molecular docking, MD simulations and ADME studies of phytoconstituents of *Plumeria alba* as potential antidiabetics

Leena Khanna[a], Mansi[a], Sangeeta Talwar[b], Neeti Misra[c], Subhash C Jain[d] & Pankaj Khanna*[c,d]

[a] University School of Basic and Applied Sciences, Guru Gobind Singh Indraprastha University, New Delhi 110 078, India

[b] Department of Chemistry, Deen Dayal Upadhyaya College, University of Delhi, New Delhi 110 078, India

[c] Department of Chemistry, Acharya Narendra Dev College, University of Delhi, New Delhi 110 019, India

[d] Department of Chemistry, University of Delhi, Delhi 110 007, India

E-mail: pankajkhanna@andc.du.ac.in, jainsc48@hotmail.com

Received 24 July 2023; accepted (revised) 25 October 2023

Diabetes mellitus is a complex endocrine disorder of global concern, associated with the development of metabolism-related complications in the body, and is spreading like an epidemic. With a variety of medical treatments available and no absolute cure for this disorder, there is a great need to search for safe and efficacious antidiabetic molecules, which can be achieved using high throughput screening protocols or *in silico* screening techniques. However, many synthetic molecules are available for the purpose, use of natural products is known to be viable owing to lesser side effects. Thus, in the present study, the phytochemical investigation of *Plumeria alba*, known for antidiabetic properties, has been carried out to isolate 12 compounds in pure form, using various chromatography and crystallization techniques. Further, the *in silico* screening for antidiabetic efficacy has been done for 22 compounds including the literature known and the above isolated ones. AutoDock 4.2 and GROMACS software have been utilized for analyzing inhibition of α-glucosidase (PDB ID: 2ZE0) through molecular docking and MD simulations. Steroids and triterpenes *viz*. lup-20(29)-ene-3-yl-hexanoate (PA-1), 4α-methyl-5α-stigmast-7,24(28)-dien-3β-ol (PA-5), 4α-methyl-5α-stigmast-7,24(28)-dien-3β-O-glucoside (PA-7), lup-20(29)-en-3-one (PA-8), 3β-hydroxy-12-ursene-28-oic acid (PA-12), β-sitosterol (L1) and β-amyrin (L3) display high binding energies from –9.80 to –9.03 kcal/mol. The physicochemical and ADME analysis have also been carried out on the best leads, using Molinspiration cheminformatics and PreADMET servers respectively, to further strengthen their suitability as α-glucosidase inhibitors.

Keywords: *Plumeria alba*, Diabetes, α-Glucosidase, Molecular docking, MD simulations

Diabetes mellitus-Type 2 is a major issue for health care industry today. It is a metabolic syndrome with high blood glucose level and occurs mainly due to oxidative stress and erratic lifestyle. Its treatment is quite complex and many symptoms are associated with it. The major risk factor is elevated postprandial hyperglycemia (PPHG) due to the action of glucosidase enzymes that help break down complex carbohydrates into monosaccharides. Human pancreatic α-amylase belongs to the family of glycoside hydrolases GH13, which can hydrolyze 1,-4- or 1,-6-bonds of α-D-glucosides and releases α-D-glucose unit. Natural products are well explored as potential sources for herbal drugs in past decades, including extensive research on the screening of natural antidiabetic agents[1,2]. However, only limited natural products have been clinically validated[3-5]. Hence, new natural antidiabetic agents are in great demand and could be explored extensively from different plant sources.

Thus, considering the current importance and our interest in natural products[6-8], we have chosen one such medicinally important Indian plant, *Plumeria alba* for phytochemical investigation and theoretical evaluation of their antidiabetic potential of its constituents. Various species of genus *Plumeria* have been known for their medicinal properties, including antidiabetic, besides its use in perfumery[9-12]. *Plumeria alba* is a small tree commonly known as white champa in India. Leaves are lanceolate to oblanceolate with white fragrant flowers and it remains in leaf for most part of the year[13]. Its bark is used as purgative, emmengogues and febrifuge and the fruit is edible with seeds possessing haemostatic properties[9,14]. The iridoids from *P. alba* leaves and stems have been found to be antibacterial against *E. coli, S. aureus* and *B. subtilis* strains[15]. The leaves also have antiarthritic potential and gastric antisecretory and cytoprotective properties[16,17]. *Plumeria alba* roots extract has been reported to have hypoglycemic activities as evaluated by oral glucose tolerance test on mice[18]. The

multiple importance of this plant inspired us to choose it for phytochemical study. However, this plant has also been scrutinized previously phytochemically and pharmacologically by various groups around the world. A wide spectrum of compounds such as triterpenes, iridoids, steroids, carbohydrates, carboxylic acids, *etc*., have been thus far isolated from the genus *Plumeria*[19-28] (Fig. 1). As many of these were known to possess antidiabetic potential[29-37], we envisaged to extensively investigate the species *P. alba*, phytochemically for more active compounds, as antidiabetics. Thus, twelve compounds have been isolated and characterized from the stems and leaves of *Plumeria alba*. These isolated compounds along with the literature known ones, have been evaluated using *in silico* tools for antidiabetic efficacy.

Materials and Methods

The stems and leaves (2kg) were collected from Jorhat, Assam. The whole material was then chopped, air dried and extracted first with cold chloroform/ methanol (1:1) and then with hot methanol using a Soxhlet apparatus.

The solvent-free cold extract was subjected to fractionation by column chromatography using petroleum ether and further eluted with petroleum ether, petroleum ether/chloroform, chloroform, chloroform/ methanol and methanol. The similar fractions were combined on the basis of their TLC behavior.

However, the solvent-free hot methanol extract was initially divided into four fractions on the basis of solubility as petroleum ether (**A**), chloroform (**B**), and acetone soluble (**C**) and remaining insoluble (**D**) fractions. Chloroform and acetone soluble fractions were found to contain more or less similar components on TLC so combined to obtain fraction (**E**) (Fig. 2). These three fractions were then separately subjected to column chromatography to obtain pure compounds (Fig. 3).

IR spectra were recorded on Shimadzu model IR-435 spectrophotometer using KBr discs. ^{1}H NMR spectra

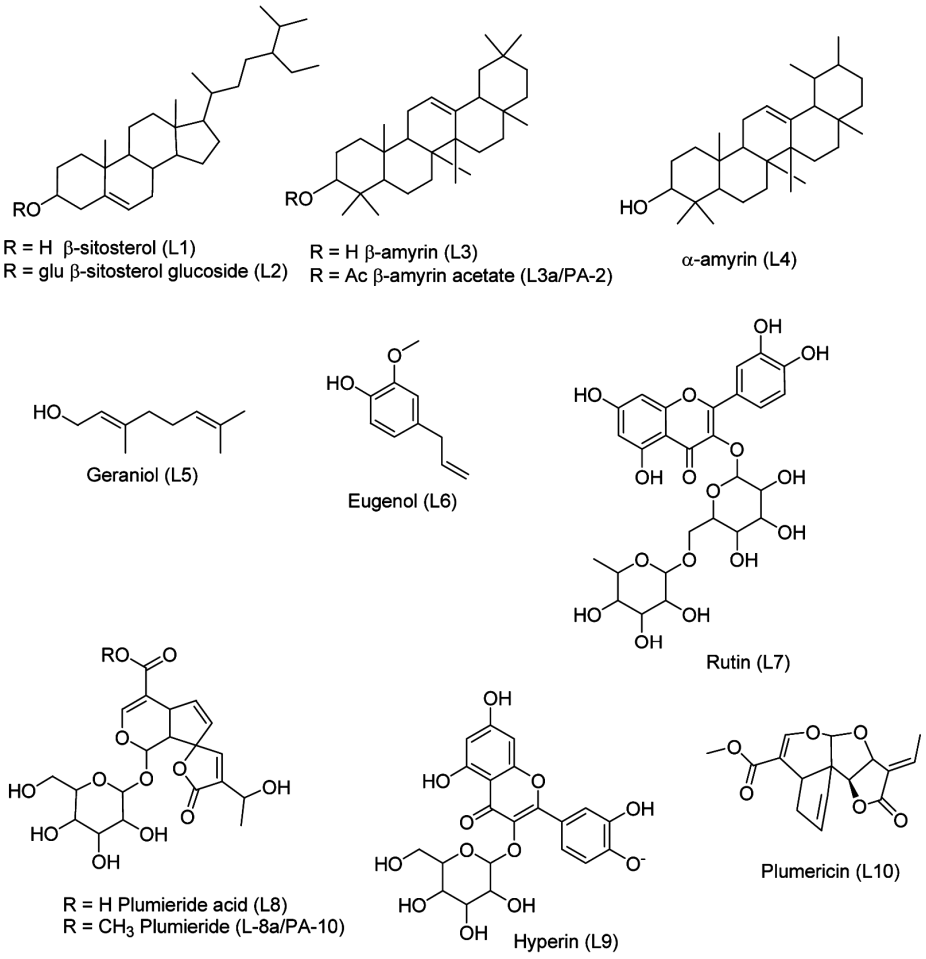

Fig. 1 — Literature known compounds from *Plumeria alba*

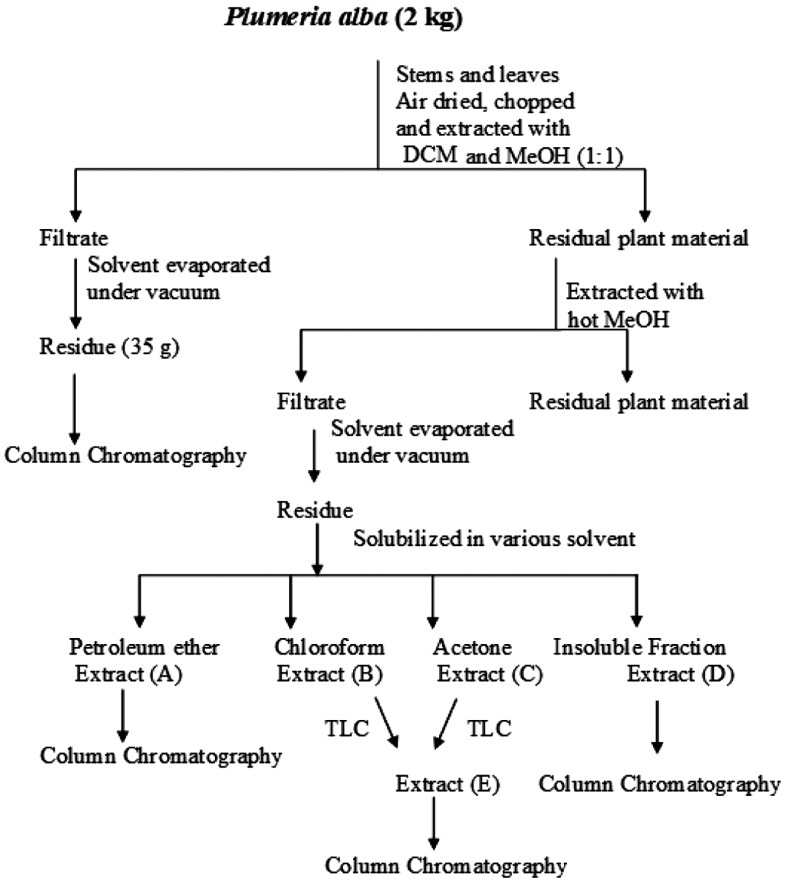

Fig. 2 — Extraction scheme for *Plumeria alba*

were recorded on Bruker AC (300 MHz) while ^{13}C NMR were recorded on Bruker AC (75.47 MHz) in deuterated solvents. Mass spectrum was taken on Jeol-JMS-DX 303 mass spectrometer. The compounds are purified by column chromatography and purity of the compounds were monitored by TLC using pre-coated aluminium-backed silica plates (E. Merck).

Molecular Docking study

The crystal structure of α-glucosidase was taken from the protein data bank (PDB ID: 2ZE0)[38,39]. The docking studies were carried out using AutoDock 4.2 software and AutoDock Tools (Graphical Interface program)[40] and the Discovery Studio Visualizer 2020 was used to make receptor and ligand files[41]. PDB files were prepared using usual procedure in AutoDock 4.2 and the grid box of 60, 60, 60 Å dimensions. Lamarckian Genetic Algorithm (LGA) was used to find the best conformers. Out of 10 conformers have been evaluated for each compound. The docked complex poses are visualized using Discovery Studio Visualizer 2020.

Molecular dynamic simulation

The best-fitted model of docked complexes of the topmost hits was subjected to GROMACS (gmx gromp, 2022) to further examine the stability of docked complexes[42,43]. The ligand topology files were generated using the PRODRG server. The GROMOS96 43a1 force field was used to simulate molecular dynamics (MD) for 1 ns with the SPC water model, used to solvate complexes in a cubic box. The system was first neutralized with sodium ions, then energy minimization was used to avoid energy clashes by using the steepest descent minimization algorithm to calm down the initial solvent and remove residual strain, with the maximum number of steps was set to 50000 and the minimization step size set to 0.01. The bond lengths inside the protein were constrained using the LINCS technique. The conventional constant temperature velocity-Verlet algorithm is used by the Macro model. Long-range electrostatic forces were used to calculate the Particle-Mesh Ewald (PME) technique, whereas the cutoff distance for short-range electrostatics was

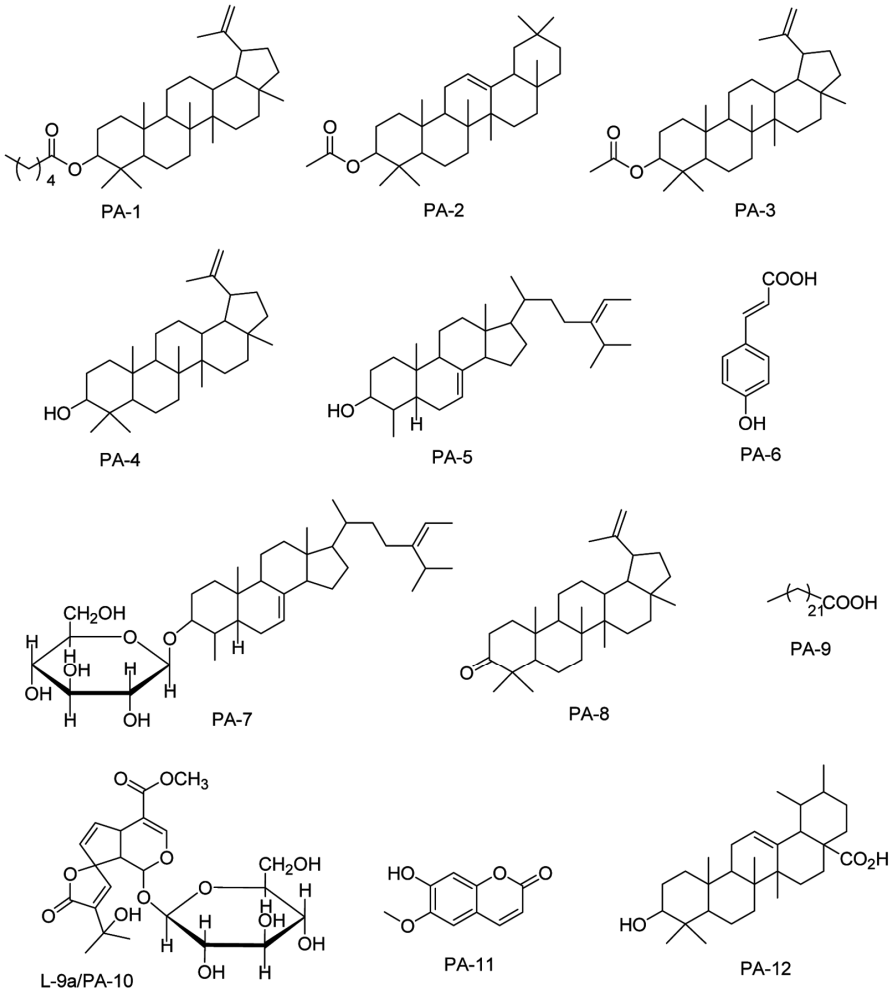

Fig. 3 — Compounds isolated from *Plumeria alba*

set to 1.2 nm. The temperature of the system remained constant at 300 K using a modified Berendsen thermostat, and the pressure was maintained at 1 atm using the Parrinello-Rahman approach, removing all system collisions. The trajectories and energy were recorded at 0.002 ps. The VMD analysis tool was used to analyze the trajectories with RMSD and RMSF values, several hydrogen bonds, and radius of gyration with the calculation of interaction energy over the simulation trajectories.

Physicochemical properties and ADME analysis

The Molinspiration cheminformatics server (www.molinspiration.com) was used for the analysis of physiochemical properties, and the PreADMET webserver was used for the evaluation of the drug-likeness, as in our earlier reports[43,44]. The Lipinski Rule of Five served as the foundation for screening the drug-likeliness of the compounds with the following parameters: LogP (octanol/water partition coefficient), TPSA (topological polar surface area), natoms (number of atoms), MW (molecular weight), Nviolations (number of violations), Nrot (number of rotatable bonds), and volume.

PreADMET web server version 2.0 was used to calculate the absorption, distribution, metabolism, excretion, and toxicity parameters in order to examine the disposition of compounds within an organism. BBB (blood-brain barrier), Caco2 levels, HIA (human intestinal absorption), MDCK cell line values, SP (skin permeability), and PPB (plasma protein binding) are among the ADME metrics. In addition, the bioactivity scores of six pharmacological classes—GPCR ligands, kinase inhibitors, ion channel modulators, nuclear receptor ligands, protease inhibitors, and enzyme targets are reported.

Results and Discussion

The extracts obtained from above scheme were subjected to column chromatography and twelve compounds have been isolated in pure form. These compounds have been identified as: lup-20(29)-ene-3-yl-hexanoate (**PA-1**), 3β-O-acetylolean-12-ene (**PA-2/L3a**, β-amyrin acetate), 3β-O-acetyl-lup-20(29)-ene (**PA-3**), lup-20(29)-ene-3β-ol (**PA-4**, lupeol), 4α-methyl-5α-stigmast-7,24(28)-dien-3β-ol (**PA-5**, α-sitosterol), *p*-hydroxy cinnamic acid (**PA-6**), 4α-methyl-5α-stigmast-7,24(28)-dien-3β-O-glucoside (**PA-7**, α-sitosterol glucoside), lup-20(29)-ene-3-one (**PA-8**, lupenone), tricosanoic acid (**PA-9**), plumieride (**PA-10**), 7-hydroxy-6-methoxy-1*H*-benzopyran-2-one (**PA-11**, scopoletin) and 3β-hydroxy-12-ursene-28-oic acid (**PA-12,** ursolic acid). All of the above compounds were identified on the basis of IR, ^{1}H NMR, ^{13}C NMR, Mass spectra and DEPT (in some cases) experiments (Supplementary information S2-S10) and also by comparing physical and spectral data with that reported in literature. This is the first report of isolation of lupenone **(PA-8)**, α-sitosterol **(PA-5)** and α-sitosterol glucoside (**PA-7**) from the genus *Plumeria*. Moreover, compounds **PA-3**, **PA-4** and **PA-6** are also the first report from *P. alba* species.

Molecular Docking Study

The antidiabetic potency of the above 22 natural products (12 newly isolated (**PA-1 - PA-12**) and 10 (**L1-L10**) already known in the literature from *P. alba*), the molecular docking study has been performed with α-glucosidase using PDB ID: 2ZE0 (Supplementary Information S11-20). However, the compounds with highest binding energies (**PA-1**, **PA-5**, **PA-7 and L1**) and interactions with protein are listed in Table 1. This crystal structure has been used earlier for identifying natural products against diabetes[38,39]. Acarbose, a well-known antidiabetic drug and an inhibitor of α-glucosidase, is used as a standard for this study. The crystal structure of α-glucosidase consists of three domains and Asp199, Glu256, Asp326 are highly conserved catalytic residues while Tyr63, His103 and His325 are the residues important for substrate binding (Fig. 4)[38].

The compound **PA-1** showed the strongest binding energy of -9.80 kcal/mol with a conventional H bond with His203 at a distance of 2.13 Å. It also shows Pi alkyl interactions with Trp268 at 4.49 Å and Phe 276 at 5.07 Å as depicted in Fig. 5. Alkyl interactions with Ala200 and van der Waal interactions with important amino acids of active site are Asp 382, Arg 411, Asp 60, His 325, Tyr 63, Asp 326, Asp 199, Phe 144, Arg 407, Ser 384, Phe 163, Asn 258, Met 229 and Ser 202 (Fig. 5). Similarly, compounds **PA-5** and **PA-7** displayed various binding interactions with the target enzyme.

MD Simulation

The molecular dynamic simulation studies of best binding compounds **PA-1**, **PA-5** and **PA-7** was done. **L1** (β-sitosterol), although having a high value of binding energy, is not included due to its already recently reported antidiabetic study[32].

Table 1 — Docking interactions and free energy of binding for lead compounds **PA-1**, **PA-5**, **PA-7** and **L1** against GH 13 α glucosidase (PDB ID: 2ZE0)

Compd	Free Energy of binding kcal/mol	Inhibition constant Ki	Interaction type	Interactions
PA-1	–9.80	65.27 nM	Van der Waals	Asp 382, Arg 411, Asp 60, His 325, Tyr 63, Asp 326, Asp 199, Phe 144, Arg 407, Ser 384, Phe 163, Asn 258, Met 229, Ser 202
			Pi Alkyl	Trp 268, Phe 276
			Alkyl	Ala 200
			Conventional Hydrogen Bond	His 203
PA-5	–9.54	101.55 nM	Van der Waals	Asn 61, Gln 167, His 103, Ala 200, Asp 199, Trp 49, Arg 197, Asn 324, Phe 282, Glu 256, Asp 60
			Pi Alkyl	Phe 163, Phe 144, Tyr 63, His 325
			Conventional H Bonding	Asp 326

(*Contd.*)

Table 1 — Docking interactions and free energy of binding for lead compounds **PA-1**, **PA-5**, **PA-7** and **L1** against GH 13 α glucosidase (PDB ID: 2ZE0) (*Contd*)

Compd	Free Energy of binding kcal/mol	Inhibition constant Ki	Interaction type	Interactions
PA-7	–9.54	101.93 nM	Van der Waals	Asn 258, Arg 197, Trp 49, Glu 256, Asp 199, Val 100, His 103, Gln 167, Ala 59, Asp 60, Phe 144, Asn 61, Arg 411, Val 383
			Pi Sigma	Tyr 63
			Alkyl	Ala 200
			Pi alkyl	Phe 282, Phe 163, His 325
			Conventional H Bonding	Arg 407, Asp 382
			Carbon Hydrogen bond	Ser 384
L1	–9.72	74.87 nM	Van der Waals	Asp 98, Glu 256, Asp 199, Trp 49, Arg 197, Phe 282, His 325, Asp 326, Asn 324, Arg 411, Arg 407, Asn 61, Ser 384, Asp 60, Asn 61, Phe 144, Asp 60, Gln 167, His 103
			Pi alkyl	Tyr 63
			Alkyl	Ala 200
			Conventional H Bonding	Asp 382
Acarbose	–4.34	662.70 uM	Van der Waals	Leu 327, Leu 285, Phe 282, Asn 324, Arg 187, Ala 200, Phe 144, Ala 59, Arg 411, Ile143, His 103
			Pi sigma	Tyr 63
			Pi lone pair	Phe 163
			Conventional H Bonding	Asp 326, Glu 256, Asp 60, Asn 61, Gln 167, His 325, Asn 258

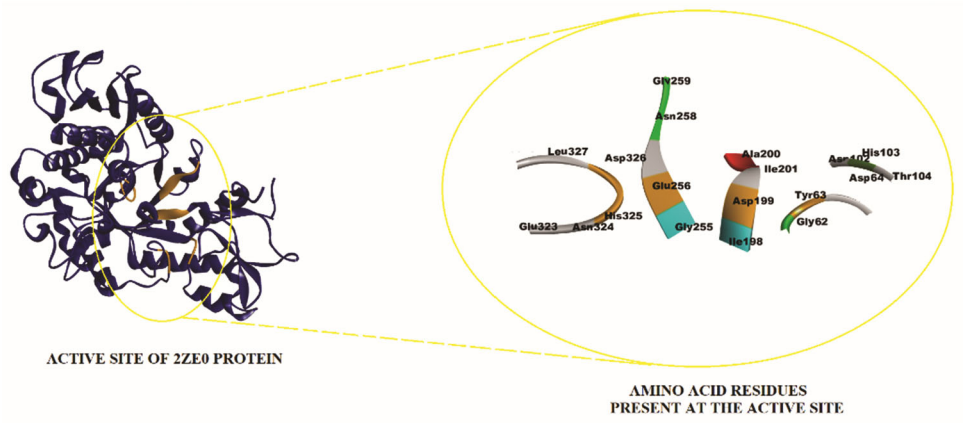

Fig. 4 — Active site of 2ZE0 with and amino acids involved

The Root Mean Square Deviation of backbone variation of protein and complex structures

The backbone of 2ZE0 protein and complex structures were plotted using the Root Mean Square Deviation (RMSD) method (Fig. 6). After 0.40 ns, all of the complexes had reached a stable state, but the protein still had minor variances. The RMSD plot of the protein structure similarly demonstrated stability before 0.40 ns, but after 0.36 ns, it became very dynamic and showed fluctuations. In the instance of complex **PA-1**, the trajectory is initially volatile, but after 0.36 ns, it becomes stable. While in the instance of complex **PA-5**, the trajectory initially stabilized and remained the same, after 0.56 ns, there was a small jump of less than 0.1 nm that quickly stabilized. The trajectory in complex **PA-7** is stable, with the same fluctuation and a tiny leap of about 0.76 ns. The RMSD fluctuations give a notion of a protein's backbone deviation. The RMSD graphic depicts the dynamic behavior of the protein structure and the

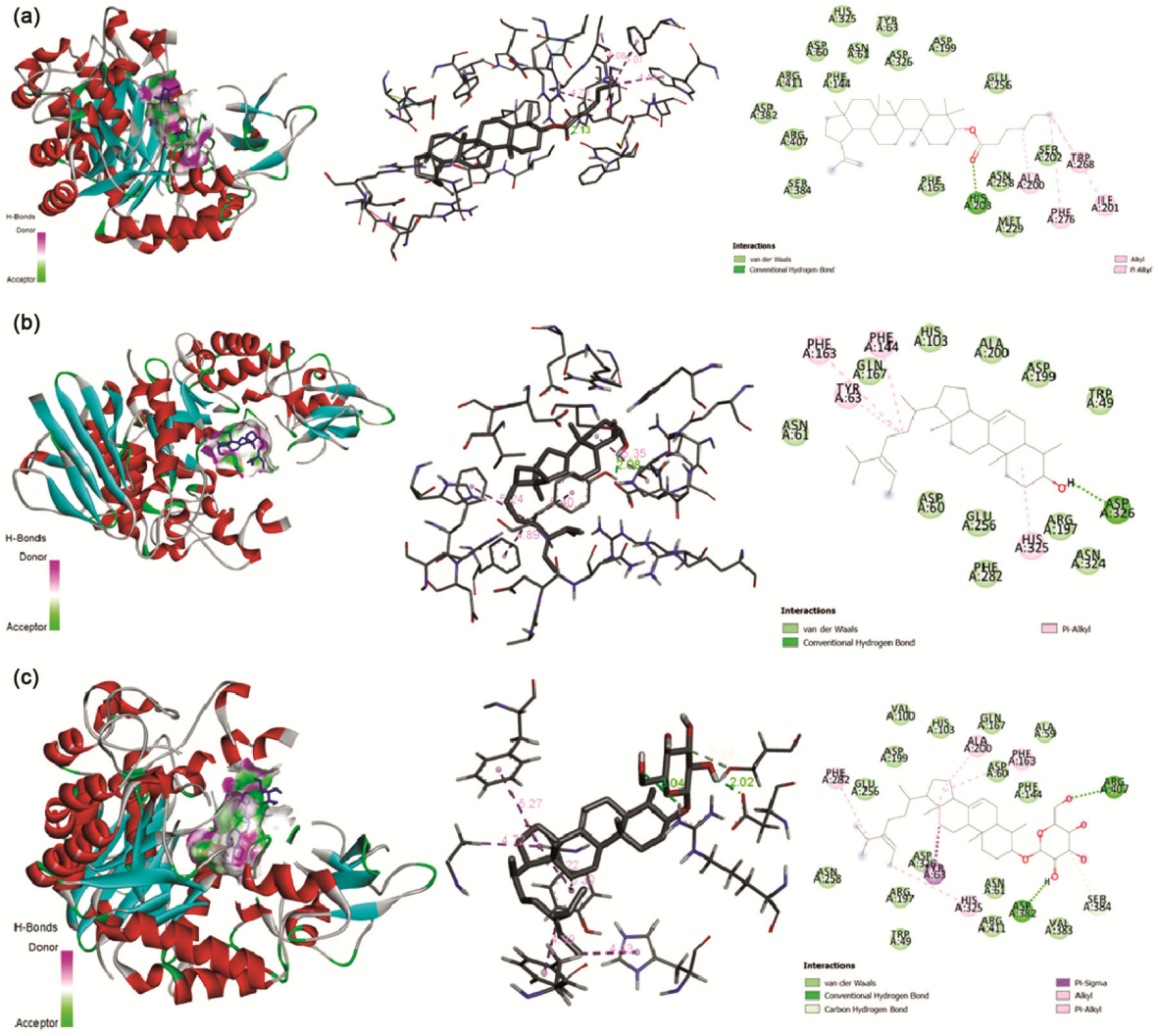

Fig. 5 — Molecular docking of 2ZE0 with a) **PA-1**, b) **PA-5** and c) **PA-7**

complex generated in this case. The plots show that **PA-5** and **PA-7** have significantly more stable plots than the protein structure, whereas all the ligand complexes (**PA-1**, **PA-5**, **PA-7**) have less variation and are thus more stable than the protein structure. Furthermore, complexes formed by the ligands **PA-1**, **PA-5**, and **PA-7** with 2ZE0 protein reduced protein flexibility and provided dynamical conformational stability.

The residue-wise fluctuations over MD trajectory

We can study the fluctuation of residual variation using Root Mean Square Fluctuation (RMSF). The variations for all of the structures are relatively similar, as can be seen (Fig. 7). Complex **PA-1**, near Phe144 residue, has a lot of variances in the F1 region. However, a change in complex **PA-5** and **PA-7**, near Ala200 to Met229 residues showed a lot of fluctuation in the F2 region. The F3 fluctuation area, *i.e*., the region near the residues Phe276 to Phe282 of the protein structure, has exhibited substantial fluctuation in the protein. The fluctuation in all of the complexes was comparable to that of the protein structure, indicating that the complexes are significantly more stable and have lower energy than the protein, which could be attributed to ligand binding.

The radius of gyration analysis

The radius of gyration (Rg) value indicates how structural variation influences the compactness of the protein after complex formation with ligands. The Rg values of folded and unfolded confirmation proteins

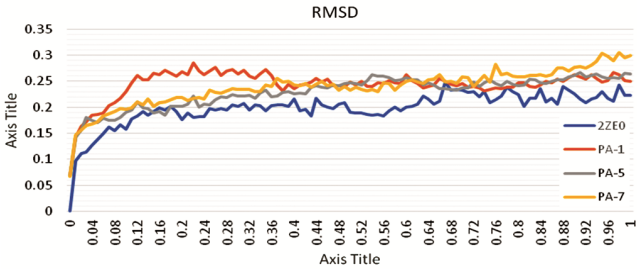

Fig. 6 — MD Simulation study of **PA-1**, **PA-5** and **PA-7**

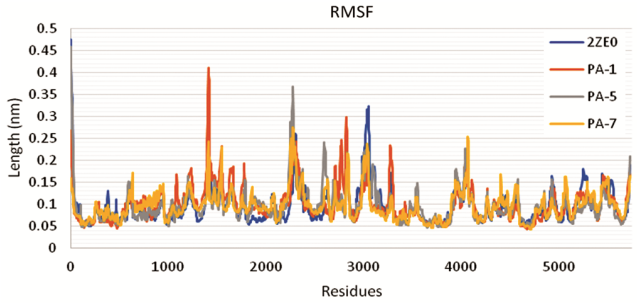

Fig. 7 — MD Simulation RMSF of **PA-1**, **PA-5** and **PA-7**

are low and high, respectively. The compactness of all the compounds, as well as the apo, was found to be fairly stable (Fig. 8). A higher Rg value meant that the protein was more flexible. Rg, both as a protein and as a complex, has shown little change. There isn't much of a difference in protein packing here. The average Rg values for structures complex **PA-1**, complex **PA-5**, and complex **PA-7** were 2.425 nm, 2.398 nm, and 2.384 nm, respectively, whereas the protein was 2.417 nm. There is not a lot of variation in Rg average values, which implies that the globularity of the complexes is not changing dramatically in comparison to protein. In complexes, a slight difference in Rg was expected.

Hydrogen bond analysis

Hydrogen bond formation is critical for understanding protein structural integrity, catalytic region, and protein-ligand interaction, as well as protein stability and conformation. The hydrogen bond interaction within the protein of all the complexes does not alter much. Protein, complex **PA-1**, complex **PA-5**, and complex **PA-7** had high average hydrogen bond values of 1029, 1023, 1038, and 1022 respectively (Fig. 9). Furthermore, the number of hydrogen bonds between protein and ligand complex structures was computed for pairings within 0.35 nm. The maximum hits for

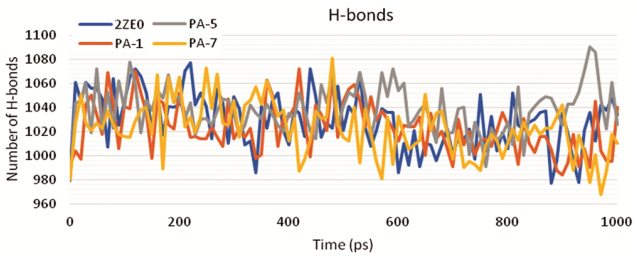

Fig. 8 — Radius of gyration of complexes of **PA-1**, **PA-5** and **PA-7** with 2ZE0 protein

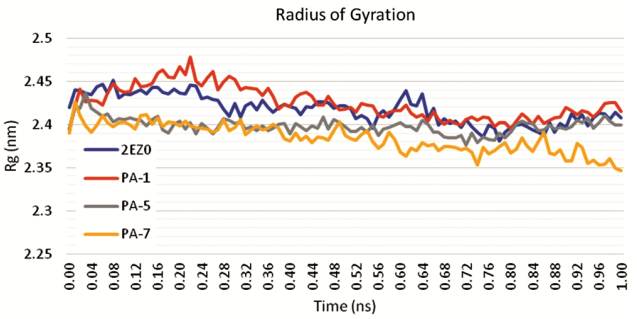

Fig. 9 — H-bonds interactions in complexes of **PA-1**, **PA-5** and **PA-7** with 2ZE0 protein

complex **PA-1** were 1 pair, while the maximum hits for complex **PA-7** were 3, but increased in value with time variation. This revealed that the ligand could make hydrogen bonds with a high frequency of occurrence. The other non-covalent interactions, on the other hand, should have aided molecule binding.

Physicochemical and ADME properties of lead compounds

In-silico physicochemical and ADME study of the compounds with highest binding energy was performed (Table 2). Oral bioavailability and drug likeliness are essential in the development of bioactive compounds. The known "Lipinski rule of five", was used to predict ADME properties, as in our earlier reports[43,44]. Besides these, for a pharmaceutical compound to be effective against a specific target, plasma protein binding (PPB) levels of around 90% are acceptable. Here, all three derivatives are within the ranges of the ADME and physicochemical parameters, demonstrating good oral bioavailability, though having one or two violations of the Lipinski rule, that are within permissible ranges. Good bioactivity scores were shown by all the derivatives.

Table 2 — Physiochemical and ADME parameters with bioactivity scores for lead compounds **PA-1**, **PA-5**, and **PA-7**

Descriptors	PA-1	PA-5	PA-7
	Physicochemical Properties		
Molecular weight (g/mol)	524.87	426.72	588.87
Number of heavy atoms	38	31	42
Number of rotatable bonds	7	5	8
Number of H-bond acceptors	2	1	6
Number of Hydrogen bond donor	0	1	4
miLogP	9.38	8.15	6.46
TPSA (Å^2)	26.30	20.23	99.38
Volume	565.32	466.89	599.01
	Drug-likeness		
Lipinski Rule of Five	2	1	2
	ADME properties		
HIA	100	100	90.973324
GI absorption	Low	low	low
Skin Permeability	–1.0696	–0.67611	–2.13272
P-glycoprotein Inhibitor	Inhibitor	Inhibitor	Inhibitor
Blood-Brain Barrier	21.3749	20.7157	5.58746
Caco2	53.5673	52.5672	25.7121
MDCK	0.0478168	2.44392	0.0793069
PPB	100	100	100
CYP_2C19_inhibition	Non	Non	Non
CYP_2C9_inhibition	Inhibitor	Inhibitor	Inhibitor
CYP_2D6_inhibition	Non	Non	Non
CYP_2D6_substrate	Non	Non	Non
CYP_3A4_inhibition	Inhibitor	Inhibitor	Inhibitor
CYP_3A4_substrate	Substrate	Substrate	Substrate
	Bioactivity Scores		
GPCR ligand	0.17	0.15	0.12
Ion channel modulator	–0.05	0.15	–0.24
Kinase inhibitor	–0.48	–0.34	–0.39
Nuclear receptor ligand	0.64	0.89	0.39
Protease inhibitor	0.10	–0.13	–0.07
Enzyme inhibitor	0.40	0.66	0.47

Conclusion

The phytochemical investigation of leaves and stems of *Plumeria alba* has been successfully performed to isolate twelve compounds in pure form. These were characterized on the basis of detailed spectral studies *viz.* IR, Mass, ^{1}H and ^{13}C NMR spectra. Major leads characterized as plumeride, *p*-coumaric acid, scopoletin, lup-20(29)-ene-3β-ol, lup-20(29)-ene-3-one, 3-acetyl lup-20(29)-ene-3β-ol, amyrin acetate, ursolic acid and α-sitosterol and its glucoside. The literature survey of the previously isolated compounds from *Plumeria alba* is also included. All these compounds showed better efficacy through *in silico* study, than antidiabetic drug acarbose, in the inhibition of α-glucosidase GH13 family enzyme, using Molecular docking and MD simulations. High binding energies from -9.80 to -9.03 kcal/mol were found in docking studies and three best leads are reported with MD simulations and ADME studies. Owing to the results obtained for many isolated and known compounds from *Plumeria alba* and the literature cited, it may be concluded as a highly potent plant for treating diabetes.

Acknowledgements

The authors would like to thank Faculty Research Grant Scheme (FRGS) 2023-24 of Guru Gobind Singh Indraprastha University and Council of Scientific and Industrial Research, for financial support. Mansi is grateful to Guru Gobind Singh Indraprastha University for providing STRF.

Conflicts of Interest

The authors declare no conflict of interest.

Supplementary Information

Supplementary information is available in the website http://nopr.niscpr.res.in/handle/123456789/58776.

References

1 Jhong C H, Riyaphan J, Lin S H, Chia Y C & Weng, C F, *Biofactors*, 41 (2015) 242.
2 Udrea A M, Pircalabioru G G, Boboc A A, Mares C, Dinache A, Mernea M & Avram S, *Biomolecules*, 11 (2021) 1692.
3 Jugran A K, Rawat S, Devkota H P, Bhatt I D & Rawal R S, *Phytother Res*, 35 (2020) 223.
4 Bharti S K, Krishnan S, Kumar A & Kumar A, *Ther. Adv. Endocrinol. Metab*, 9 (2018) 81.
5 Mukherjee P K, Kar A, Banerjee S & Katiyar C K, *Annu Rep Med Chem*, 55 (2020) 373.
6 Sehgal N, Gupta A, Valli R K, Joshi S D, Mills J T, Hamel E, Khanna P, Jain S C, Thakur S S & Ravindranath V, *Proc Nat Acad Sci*, 109 (2012) 3510.
7 Panda S S, Girgis A S, Prakash A, Khanna L, Khanna P, Shalaby E S M, Fawzy N G & Jain S C, *Heliyon*, 4 (2018) e00951.
8 Upadhyay R K, Rohatgi L, Chaubey M K & Jain S C, *J Agric Food Chem*, 54 (2006) 9747.
9 Barry A, Enade I & Maywan H, *J Med Plants Res*, 14 (2020) 544.
10 Semenya S, Potgieter M, Erasmus L, *J. Ethnopharmacol*, 141 (2012) 440.
11 Sharma G, Chahar M K, Dobhal S, Sharma N, Sharma T C, Sharma M C, Joshi Y C & Dobhal M P, *Chem Biodiversity*, 8 (2011) 1357.
12 Joulain D, *Chem Biodiversity*, 5 (2008) 896.
13 Chopra R N, Nayar S L & Chopra I L, *Glossary of Medicinal Plants*, (New Delhi: CSIR) 1956.
14 Kalita D & Saikia C N, *Bioresour Technol*, 92 (2004) 219.
15 Afifi M S, Salama O M, Gohar A A & Marzouk A M, *Bull Pharm Sci*, 29 (2006) 215.
16 Choudhary M, Kumar V, Gupta P & Singh S, *BioMed Res Int*, 2014 (2014) 1.
17 Choudhary M, Kumar V & Singh S, *J Integr Med*, 12 (2014) 42.
18 Kadebe Z T, Metowogo K, Bakoma B, Lawson-Evi S P, Eklu-Gadegbeku K, Aklikokou K & Gbeassor M, *Trop J Pharm Res,* 15 (2016) 87.
19 Kamariah A S, Lim L B L, Baser K H C, Ozek T & Demirci B, *Flavour Fragrance J,* 14 (1999) 237.
20 Tomosaka H, Koshino H, Tajika T & Omata S, *Biosci Biotechnol Biochem*, 65 (2001), 1198.
21 Pino J A, Ferrer A, Alvarez D & Rosado A, *Flavour Fragrance J*, 9(1994), 343.
22 Omata A, Nakamura S, Hashimoto S & Furukawa K, *Flavour Fragrance J*, 7(1992), 33.
23 Rangaswami S & Rao E V, *Proc Ind Acad Sci,* 52A (1960) 173.
24 Mahran G H, Abdel-Wahab S M & Ahmed M S, *Planta Med*, 25(1974) 226.
25 Bramadhayalaselvam A, Hussain A J, Mathuram V, Rao R B & Patra A, *Fitoterapia (Milano)*, 68 (1997) 554.
26 Marimuthu S, Shah G L & Kothari I L, *Indian Bot Contactor*, 3 (1986) 73.
27 Gunasingh C B G & Nagarajan S, *Ind J Pharm Sci*, 42 (1980) 178.
28 Mahran G H, Abdel-Wahab S M & Ahmed M S, *Egyptian J Pharm Sci*, 5 (1974) 43.
29 Ghorbani A, *Biomed Pharmacother*, 96 (2017) 305.
30 Habtemariam S & Lentini G, *Mini Rev Med Chem*, 15 (2015) 524.
31 Babu S & Jayaraman S, *Biomed Pharmacother*, 131 (2020) 110702.
32 Ravi L, Girish S, D'Souza S R, Sreenivas B K A, Kumari G R S, Archana O, Kumar K A & Manjunathan R, *J Biomol Struct Dyn*, (2023), (https://doi.org/10.1080/07391102.2023.2186703).
33 Lee H A, Kim M J & Han J S, *Toxicol Res (Camb)*, 10 (2021) 495.
34 Santos F A, Frota J T, Arruda B R, de Melo T S, Silva A A D, Brito G A, Chaves M H & Rao V S, *Lipids Health Dis*, 11 (2012) 98.
35 Carvalho R P R, Lima G D de A & Machado-Neves M, *Pharmacol Res*, 165 (2021) 105315.
36 Al-Kury L T, Abdoh A, Ikbariah K, Sadek B & Mahgoub M, *Molecules*, 27 (2022) 182.
37 Verma N, Amresh G, Sahu P K, Mishra N, Rao Ch V & Singh A P, *Indian J Exp Biol*, 51 (2013) 65.
38 Shirai T, Hung V S, Morinaka K, Kobayashi T & Ito S, *Proteins*, 73 (2008) 126.
39 Akhtar N, Jafri L, Green B D, Kalsoom S & Mirza B, *Front Pharmacol*, 9 (2018) 1376.
40 Morris G M, Huey R, Lindstrom W, Sanner M F, Belew R K, Goodsell D S & Olson A J, *J Comput Chem*, 3 (2009) 2785.
41 Dassault Systèmes BIOVIA, Discovery Studio Visualizer, R2 client, *San Diego: Dassault Systèmes* (2020).
42 Gorai S, Junghare V, Kundu K, Gharui S, Kumar M, Patro B S, Nayak S K, Hazra S & Mula S, *Chem Med Chem*, 17 (2022) 1.
43 Mansi, Khanna P, Gupta D, Yadav S & Khanna L, *J Biomol Struct Dyn*, (2022) (https://doi.org/10.1080/07391102.2022.2145368).
44 Singhal S, Khanna P, Misra N & Khanna L, *Chem Select*, 6 (2021) 4112.